Biogeosciences Discuss., 11, 10537–10569, 2014
www.biogeosciences-discuss.net/11/10537/2014/
doi:10.5194/bgd-11-10537-2014

Biogeosciences
Discussions
Open Access

iMarNet: an ocean biogeochemistry model inter-comparison project within a common physical ocean modelling framework

L. Kwiatkowski[1,2], A. Yool[3], J. I. Allen[4], T. R. Anderson[3], R. Barciela[5], E. T. Buitenhuis[6], M. Butenschön[3], C. Enright[6], P. R. Halloran[7], C. Le Quéré[6], L. de Mora[4], M.-F. Racault[4], B. Sinha[3], I. J. Totterdell[5], and P. M. Cox[1]

[1]College of Engineering, Mathematics and Physical Sciences, University of Exeter, Exeter, EX4 4QF, UK
[2]Department of Global Ecology, Carnegie Institution for Science, 260 Panama Street, Stanford, California, 94305, USA
[3]National Oceanography Centre, University of Southampton Waterfront Campus, European Way, Southampton, SO14 3ZH, UK
[4]Plymouth Marine Laboratory, Prospect Place, West Hoe, Plymouth, PL1 3DH, UK
[5]Hadley Centre, Met Office, Exeter, EX1 3PB, UK
[6]Tyndall Centre for Climate Change Research, School of Environmental Sciences, University of East Anglia, Norwich, UK
[7]College of Life and Environmental Sciences, University of Exeter, Exeter, EX4 4RJ, UK

Received: 5 June 2014 – Accepted: 21 June 2014 – Published: 10 July 2014

Correspondence to: L. Kwiatkowski (lkwiatkowski@carnegiescience.edu)

Published by Copernicus Publications on behalf of the European Geosciences Union.

Abstract

Ocean biogeochemistry (OBGC) models span a wide range of complexities from highly simplified, nutrient-restoring schemes, through nutrient-phytoplankton-zooplankton-detritus (NPZD) models that crudely represent the marine biota, through to models that represent a broader trophic structure by grouping organisms as plankton functional types (PFT) based on their biogeochemical role (Dynamic Green Ocean Models; DGOM) and ecosystem models which group organisms by ecological function and trait. OBGC models are now integral components of Earth System Models (ESMs), but they compete for computing resources with higher resolution dynamical setups and with other components such as atmospheric chemistry and terrestrial vegetation schemes. As such, the choice of OBGC in ESMs needs to balance model complexity and realism alongside relative computing cost. Here, we present an inter-comparison of six OBGC models that were candidates for implementation within the next UK Earth System Model (UKESM1). The models cover a large range of biological complexity (from 7 to 57 tracers) but all include representations of at least the nitrogen, carbon, alkalinity and oxygen cycles. Each OBGC model was coupled to the Nucleus for the European Modelling of the Ocean (NEMO) ocean general circulation model (GCM), and results from physically identical hindcast simulations were compared. Model skill was evaluated for biogeochemical metrics of global-scale bulk properties using conventional statistical techniques. The computing cost of each model was also measured in standardised tests run at two resource levels. No model is shown to consistently outperform or underperform all other models across all metrics. Nonetheless, the simpler models that are easier to tune are broadly closer to observations across a number of fields, and thus offer a high-efficiency option for ESMs that prioritise high resolution climate dynamics. However, simpler models provide limited insight into more complex marine biogeochemical processes and ecosystem pathways, and a parallel approach of low resolution climate dynamics and high complexity biogeochemistry is desirable in order to provide additional insights into biogeochemistry–climate interactions.

1 Introduction

Ocean biogeochemistry is a key part of the Earth System: it regulates the cycles of major biogeochemical elements and controls the associated feedback processes between the land, ocean and atmosphere. As a result, changes in ocean biogeochemistry can have important implications for climate (Reid et al., 2009). Marine ecosystems are affected by both the direct human exploitation of the seas and the indirect anthropogenic environmental change (Jackson et al., 2001), particularly through climate-induced changes in physical properties and CO_2-induced ocean acidification. Understanding and quantifying the response of ocean biogeochemistry to global changes and their feedbacks with the Earth System is essential to improve our capacity to maintain ecosystem services this century and beyond.

With the recent publication of the Intergovernmental Panel on Climate Change (IPCC) 5th Assessment Report (AR5), global efforts are already underway to develop the next generation of Earth System Models (ESMs) to support climate policy development and any further IPCC Assessment Report. OBGC coupled to ESMs can help address a series of overarching scientific questions: how will the ocean contribute to atmospheric trace gas composition (e.g. CO_2, CH_4, N_2O, DMS) in a changing climate? Are there tipping points in marine biogeochemistry (e.g. oceanic anoxic events, methane hydrate release) that could be triggered by a changing climate? Are there interactions between ESM processes and society's management of resources (e.g. fisheries, land use, agriculture) in the marine environment? Furthermore, as ESMs are increasingly being evaluated based on their capacity to understand past variability (Braconnot et al., 2012), further questions might include: What controlled the variations in atmospheric trace gas over the geological past including those measured by isotopes?

For an anticipated 6th IPCC assessment report it is generally considered that these global-scale questions, with direct implications for climate policies, will again be the main focus of ocean biogeochemical models within ESMs. In addition, the ESM model archive produced by the IPCC is increasingly being used for example by some activ-

Title Page
Abstract Introduction
Conclusions References
Tables Figures
◀| |▶
◀ ▶
Back Close
Full Screen / Esc
Printer-friendly Version
Interactive Discussion

ities within the Inter-Sectoral Impact Model Intercomparison Project (http://www.pik-potsdam.de/research/climate-impacts-and-vulnerabilities/research/rd2-cross-cutting-activities/isi-mip/scientific-publications) to address socioeconomically-directed questions such as: how will climate change affect oceanic primary production (e.g. Bopp et al., 2013), fisheries (Barange et al., 2014; Cheung et al., 2012), and harmful algal and jellyfish blooms (e.g. Codon et al., 2013)? What is the potential for geoengineering schemes such as ocean fertilisation (Buesseler and Boyd, 2003) and alkalinity addition (Kheshgi, 1995) to affect the climate system, and how do they affect the rest of the Earth System?

Within the UK, the Integrated Global Biogeochemical Modelling Network (iMarNet) project aims to advance the development of ocean biogeochemical models through collaboration between existing modelling groups at Plymouth Marine Laboratory (PML), National Oceanography Centre (NOC), University of East Anglia (UEA) and the Met Office-Hadley Centre (UKMO). As part of iMarNet we conducted an intercomparison of 6 current UK models, to help inform the selection of a baseline OBGC model for the next UK Earth System Model (UKESM1). This intercomparison focused on model skill at reproducing global-scale bulk properties – such as nutrient and carbon distributions – that broadly characterise the activity of marine biota (and, thus, the carbon cycle) in the ocean. To limit the role of errors originating with modelled physics, all of the examined model simulations were performed within the same physical ocean GCM, under the same external forcing and following the same experiment protocol. As all of the models examined have been previously published, our analysis does not include an assessment of their underlying biological fidelity (i.e. the extent to which structures, parameterisations and parameter sets of candidate models are a priori realistic). However, while primarily focused on model skill, the intercomparison also considers the computational cost of the models in relation to the realism that they offer.

2 Method

2.1 Experimental design

All participating models made use of a common version (v3.2) of the NEMO physical ocean general circulation model (Madec, 2008) coupled to the Los Alamos sea-ice model (CICE) (Hunke and Lipscomb, 2008). A Flexible Configuration Management (FCM) branch of this version was created, and all biogeochemical models were implemented in parallel within this branch and run separately.

Simulations were initialised at year 1890 from an extant physics-only spin-up (ocean and sea-ice), to minimise undesirable transient behaviour in ocean circulation. In terms of ocean biogeochemistry, all model runs made use of a common dataset of three-dimensional fields for the initialisation of major tracers. Nutrients (nitrogen, silicon and phosphorus) and dissolved oxygen in this dataset were drawn from the World Ocean Atlas 2009 (Garcia et al., 2010a, b), while dissolved inorganic carbon (DIC) and alkalinity were drawn from the Global Ocean Data Analysis Project (GLODAP) (Key et al., 2004). GLODAP does not include a DIC field that is directly valid for 1890, so a temporally-interpolated field was produced based on GLODAP's "pre-industrial" (i.e. ~ 1800) and "1990s" fields of DIC. As there is currently no comprehensive spatial dataset of the micronutrient iron, participating models were permitted to make use of different initial distributions of iron (typically those routinely used by the models in other settings). All other biogeochemical fields (e.g. plankton, particulate or dissolved organic material) were initialised to arbitrary small initial conditions.

After initialisation at 1890, the models were run for 60 years (1890–1949 inclusive) under the so-called "normal year" of version 2 forcing for common ocean-ice reference experiments (CORE2-NYF; Large and Yeager, 2009). Subsequently, the models were run under transient, interannual forcing from the same dataset (CORE2-IAF) for a further 58 years (1950–2007 inclusive). CORE2 provides observationally derived geographical fields of downwelling radiation (separate long- and short-wave), precipitation (separate rain and snow), and surface atmospheric properties (temperature, specific humidity and winds), and is used in conjunction with bulk formulae to calculate net heat, freshwater and momentum exchange between the atmosphere and the ocean.

2.2 Candidate model structures

The models evaluated within this study vary significantly in biological complexity. The key features of the participating models are summarized below:

HadOCC (Palmer and Totterdell, 2001): the Hadley Centre Ocean Carbon Cycle model (HadOCC) model is a simple NPZD (Nutrient, Phytoplankton, Zooplankton, Detritus) representation that uses N nutrient as its base currency but with coupled flows of C, alkalinity and O_2. The model was the ocean biogeochemistry component of the UK Met Office's HadCM3 climate model, and was used for the first ever fully coupled carbon-climate study (Cox et al., 2000).

Diat-HadOCC (Halloran et al., 2010): is a development of the HadOCC model which includes two phytoplankton classes (diatoms and "other phytoplankton") and representations of the Si and Fe cycles, as well as a dimethyl sulphide (DMS) sub-model for cloud feedbacks. The model is the ocean biogeochemistry component of HadGEM2-ES (Collins et al., 2011), the UK Met Office's Earth System model used to run simulations for CMIP5 and the Intergovernmental Panel on Climate Change (IPCC) 5th Assessment Report (AR5).

MEDUSA-2 (Yool et al., 2011, 2013): Model of Ecosystem Dynamics, nutrient Utilisation, Sequestration and Acidification (MEDUSA) is an "intermediate complexity" plankton ecosystem model designed to incorporate sufficient complexity to address key feedbacks between anthropogenically-driven changes (climate, acidification) and oceanic biogeochemistry. MEDUSA-2 resolves a size-structured ecosystem of small (nanophytoplankton and microzooplankton) and large (microphytoplankton and mesozooplankton) components that explicitly includes the biogeochemical cycles of N, Si and Fe nutrients as well as the cycles of C, alkalinity and O_2. As such, MEDUSA-2 is broadly similar in structure to Diat-HadOCC, but includes several more recent parameterisations.

PlankTOM6 and PlankTOM10 (Le Quéré et al., 2005): PlankTOM is a Dynamic Green Ocean Model (DGOM) that represents lower-trophic marine ecosystems based on Plankton Functional Types (PFTs). A hierarchy of PlankTOM models exists that vary in the number of PFTs resolved. Two members drawn from this stable were used in iMarNet. PlankTOM6 includes six PFTs – diatoms, coccolithophores, mixed-phytoplankton, bacteria, protozooplankton and mesozooplankton – while PlankTOM10 includes an additional four PFTs – Nitrogen-fixers, *Phaeocystis*, picophytoplankton and macrozooplankton (Le Quéré et al., 2005; Buitenhuis et al., 2013). The models include the marine cycles of C, N, O_2, P, Si, a simplified Fe cycle, and three types of detrital organic pools including their ballasting properties and estimates the air–sea fluxes of CO_2, O_2, DMS, and N_2O. PlankTOM6 and PlankTOM10 were developed by an international community of ecologists and modellers to quantify the interactions between climate and marine biogeochemistry, particularly those mediated through CO_2. They make use of extensive synthesis of data for the parameterisation of growth rates of PFTs (e.g. Buitenhuis et al., 2006, 2010) and for the model evaluation (Buitenhuis et al., 2013).

ERSEM (Baretta et al., 1995; Blackford et al., 2004): European Regional Seas Ecosystem Model (ERSEM) is a generic lower-trophic level/model designed to represent the biogeochemical cycling of C and nutrients as an emergent property of ecosystem interaction. The ecosystem is subdivided into three functional types: producers (phytoplankton), decomposers (bacteria) and consumers (zooplankton), and then further subdivided by trait (size, silica uptake) to create a foodweb. Physiological (ingestion, respiration, excretion and egestion) and population (growth, migration and mortality) processes are included in the descriptions of functional group dynamics. Four phytoplankton (picophytoplankton, nanophytoplankton, diatoms and non-siliceous macrophytoplankton), three zooplankton (microzooplankton, heterotrophic nanoflagellates and mesozooplankton) and one bacteria are represented, along with the cycling of C, N, P, Si and O_2 through pelagic (Blackford et al., 2004) and benthic (Blackford, 1997) ecosystems. ERSEM is used for shelf seas water quality monitoring and climate impact assessment, has been coupled to fisheries models (e.g. Barange et al., 2014), and is run operationally by the UK Met Office (e.g. Siddorn et al., 2007).

The representation of biogeochemical cycles and the marine biology in each model are summarized in Tables 1 and 2 respectively.

2.3 Model evaluation

Assessment against observational datasets was made for a set of bulk ocean biogeochemical properties that were common across all models: $p\mathrm{CO_2}$, alkalinity, dissolved inorganic carbon (DIC), dissolved inorganic nitrogen (DIN), chlorophyll, primary production and dissolved oxygen ($\mathrm{O_2}$). In all cases, model results were regridded to the same geographical grid (World Ocean Atlas) and model skill was assessed through statistical techniques such as global surface field standard deviation and spatial pattern correlation coefficients. In the biogeochemical regions of the North Atlantic, Equatorial Pacific and Southern Ocean, depth profiles of model outputs were also assessed against observations within the top 1000 m of the water column.

Observational fields used within the model intercomparison are comprised of World Ocean Atlas 2009 DIN and $\mathrm{O_2}$ (Garcia et al., 2010a, b), SeaWiFS chlorophyll (O'Reilly et al., 1998) and $p\mathrm{CO_2}$ (Takahashi et al., 2009). Because of its biogeochemical importance, and the diversity in published estimates, observational primary production is an average of three empirical models: Behrenfeld and Falkowski (1997), Carr et al. (2006) and Westberry et al. (2008) – which are all estimates derived from satellite ocean colour and SST. The observational fields of chlorophyll and primary production used here represent averages over the 2000–2004 time period. This same period is used throughout the following analysis as a standard interval except in the case of DIC and alkalinity, which are analysed over the mean 1990–1999 period corresponding to the GLODAP climatology.

These fields were selected for several reasons. Firstly, they are ocean or biogeochemical bulk properties for which there are global-scale observations. Secondly, these fields broadly represent foundational aspects of marine biogeochemical cycles. For instance, nutrients play a critical role in regulating the distribution and occurrence of marine plankton, while primary production by phytoplankton is the biogeochemical pathway through which the vast majority of marine ecosystems ultimately obtain energy. Thirdly, the measurement of these fields is relatively well-defined with long-established standard methodologies. Properties that are directly related to biological entities, for instance biomass abundances, can be less precisely defined, difficult to match up with modelled quantities, or even absent from some models examined here. That said, the observational field of global scale primary production used here has a relatively high uncertainty because it is drawn from three methodologies which exhibit a large range (cf. Yool et al., 2013). Finally and in part related to preceding points, the examined properties are those which, if modelled poorly, legitimately cast doubt over the wider utility of a biogeochemical model in an earth systems context. Model results always depart from observations, but systematic disagreement with these basic observations is strongly suggestive of problems with process representation within a model. The model comparison focuses on the mean and seasonal cycle. It does not include evaluation of variability over interannual or longer timescales, in part because of limited data availability.

3 Results

3.1 Model skill assessment

3.1.1 Surface fields

Figures 1–3 (and Supplement Figs. S1–S4) show annual average fields from each of the models for a series of ocean properties, together with comparable observational fields. The figures also include a panel that shows the corresponding model-observation Taylor diagram (Taylor, 2001). These illustrate both the correlation between (circumference axis) and relative variability (radial axis) of model and observations, such that models more congruent with observations generally appear closer to the reference marker on the x-axis of the diagram (Jolliff et al., 2009).

Figure 1 shows annual average surface $p\text{CO}_2$ fields for both models and observations, with correlation coefficients ranging from $r = 0.01$ to $r = 0.68$ (Takahashi et al., 2009). In general, the simpler models (HadOCC, Diat-HadOCC and MEDUSA-2) better capture the global spatial pattern of $p\text{CO}_2$ ($r = 0.54$ to $r = 0.68$), but they overestimate the standard deviation in global surface $p\text{CO}_2$ by up to a factor of 2. This overestimation of the variance in global surface $p\text{CO}_2$ is a result of high modelled $p\text{CO}_2$ values in the equatorial Pacific and in particular the Eastern equatorial Pacific. In contrast, the more complex models (PlankTOM6, PlankTOM10 and ERSEM) perform considerably worse in terms of capturing global spatial patterns of surface ocean $p\text{CO}_2$. In particular, all three models underestimate the observed high $p\text{CO}_2$ values along the equatorial Pacific ocean as well as the high coastal $p\text{CO}_2$ values in that region, opposite to the bias found in simpler models. However, the PlankTOM models overall show comparable standard deviations in mean global surface $p\text{CO}_2$ to that seen in observations.

Figure 2 illustrates model performance for annual average surface dissolved inorganic nitrogen (DIN) concentrations. Here, all models capture global patterns relatively well, with correlation coefficients > 0.8, in part because of the initialisation from observations in 1890. The model with the highest spatial pattern correlation coefficient is ERSEM, although it slightly underestimates the global variability of DIN. The other models have lower spatial pattern correlation coefficients and generally overestimate the global variability of DIN. PlankTOM6 performs below other models, while PlankTOM10 has similar performance as the simpler models. In general, aside from ERSEM and PlankTOM10, most models show elevated Pacific DIN, with the simpler models, MEDUSA-2 in particular, exhibiting high equatorial anomalies. Finally, while ERSEM shows good agreement throughout most of the world ocean, both the North Atlantic and North Pacific show anomalously low annual average DIN concentrations.

Figure 3 shows low correlation ($r < 0.5$) for annual surface chlorophyll concentrations for all models. The models with the highest correlation coefficients are PlankTOM10

(0.49) followed by MEDUSA-2 (0.36). All other models have correlation coefficients < 0.2. Anomalously high chlorophyll values in the equatorial Pacific and, especially, the Southern Ocean significantly elevate the spatial variability of Diat-HadOCC above that of observations (and all other models). More generally, with the exception of PlankTOM10, all of the models show some degree of excess chlorophyll in the Southern Ocean, with Diat-HadOCC exhibiting very high concentrations in this relatively unproductive region.

In addition to the ocean properties shown in Figs. 1–3, complementary figures for alkalinity, DIC, primary production and oxygen can be found in the Supplement (Figs. S1–S4). In each case, global annual average fields are shown together with the corresponding Taylor diagram.

Table 3 shows the correlation coefficients and standard deviations normalised relative to observations of the models for all seven of the ocean properties (six surface fields plus depth-integrated primary production). These are additionally colour-coordinated according to the rank order of model performance, and the range of correlation coefficients over all of the models is shown for each field. As already suggested above, model performance varies both between fields and between models. All models perform consistently and relatively well for DIN, DIC and, especially, oxygen, in part because of the "memory" of initial distributions. Model performance varies more widely for $p\text{CO}_2$ and primary production and varies most widely for chlorophyll, although it is consistently poor across all models. The excellent performance of all models for surface oxygen reflects the dominance of temperature-based solubility and air–sea gas exchange over biological activity for this ocean property.

Figure 4 summarises Table 3 by showing the distribution of performance rankings (both correlation coefficients and normalised standard deviations) across the selected fields for each model, i.e. the number of first, second, etc., rankings for each model. No model is shown to consistently outperform or underperform all other models across all metrics. Indeed all models perform best in at least one field metric, and similarly all models perform worst in at least one field metric. There is little discernable relationship between model complexity and model performance. Indeed Table 3 shows that for 5 out of 7 fields the best performing model in terms of correlation coefficients is a simpler model (i.e. HadOCC, Diat-HadOCC or MEDUSA-2) and for 5 out of 7 fields the best performing model in terms of normalised standard deviations is a more complex model (i.e. PlankTOM6, PlankTOM10 or ERSEM).

These findings in annual average model performance are found to be consistent when examined at monthly timescales (Supplement Fig. S5).

3.1.2 Depth profiles

While the majority of biological activity in the ocean is concentrated in its surface layers, biogeochemical fields in the deep ocean have a complex structure created through the interaction of ocean physics with biologically-mediated processes such as export and remineralisation. As such, model performance cannot be solely assessed from surface fields of ocean BGC properties. To examine this, Figs. 5 and 6 show the annual average depth profiles of DIC and alkalinity for three important regions: the North Atlantic (Atlantic 0–60° N), Southern Ocean (≥ 60° S) and Equatorial Pacific (Pacific Ocean 15° S–15° N).

In Fig. 5, all models are shown to capture the DIC profile in the Equatorial Pacific though HadOCC, Diat-HadOCC and MEDUSA-2 are somewhat closer to observations than ERSEM and the PlankTOM models. A similar situation is seen in the North Atlantic where the depth profiles of MEDUSA-2, HadOCC and Diat-HadOCC are closest to observations, although surface agreement is greater than that at depth. All models are shown to perform relatively poorly in the Southern Ocean, with much shallower gradients with depth than observations. HadOCC, Diat-HadOCC and ERSEM show gradients that are marginally closer to that observed, but all of the models consistently fail to reproduce the observed $> 100\,\mathrm{mmol\,m^{-3}}$ surface–1000 m increase. This common problem of vertical homogeneity between the models suggests that the cause lies with ocean physics deficiencies in this region.

The annual average depth profiles of alkalinity are shown in Fig. 6. Again, and for the same reasons, no model performs well at capturing the depth profile observed in the Southern Ocean. In the North Atlantic, HadOCC and Diat-HadOCC are closer to observations while ERSEM and, particularly, MEDUSA-2 are further away from observations (but in opposite directions). In the Equatorial Pacific all of the models have similar alkalinity values at depth but diverge from observations towards the surface. The near-surface depth profiles in HadOCC, Diat-HadOCC and MEDUSA-2 are closest to observations in that region. Alkalinity shows very little variability with depth in the PlankTOM6, PlankTOM10 and ERSEM models and is higher than observations in near-surface waters ($> 100\,\mathrm{meq\,m^{-3}}$). This excess alkalinity may explain the broadly lower $p\mathrm{CO}_2$ values visible in this region in Fig. 1.

The depth profiles of DIN and O_2 are given in the Supplement (Figs. S6–S7).

3.2 Computational benchmarking

Computational timing tests were carried-out relative to the ocean component of the HadGEM3 (Hewitt et al., 2011) model (ORCA1.0L75), on standard configurations of 128 and 256 processors on an IBM Power7 machine (MONSooN). As would be intuitively expected, the cost of candidate ocean biogeochemical models is found to be higher for models with more tracers regardless of the number of processors used. While there are deviations in both directions between the models, broadly there is a linear relationship between number of model tracers and compute cost (Supplement Fig. S7). This unsurprisingly reflects the significant cost of performing ocean physics operations on biogeochemical tracers.

Using ERSEM (the computationally most expensive model) increases computational cost approximately 6-fold relative to HadOCC when 128 processors are used. This relative increase in computational cost is reduced to approximately 4.5-fold when 256 processors are used. PlankTOM10 has the greatest relative reduction (36.6 %) in computational cost when run on 256 processors as opposed to 128, although this model would still increase the total cost of the ocean component by a factor of 5 relative to a physics-only ocean, compared to a factor of 1.5 for HadOCC (Table 4).

4 Discussion

Our model comparison suggests that for global annual average surface fields, global monthly average surface fields and annual average depth profiles in three oceanographic regions there is little evidence that increasing the complexity of OBGC models leads to improvements in the representation of large scale ocean patterns of bulk properties. In some cases, the comparison suggests that simpler OBGC are closer to observations than intermediate or complex models for the standard assessment metrics used here.

The biologically simpler models of HadOCC, Diat-HadOCC and MEDUSA-2 are shown to generally have higher global spatial pattern correlation coefficients of $p\mathrm{CO}_2$, DIC and alkalinity at both annual and monthly temporal resolution (Fig. 1, Supplement Fig. S5 and Table 3). The more complex models of PlankTOM6, PlankTOM10 and, in the case of DIC, ERSEM, have annual and monthly standard deviations that are generally closer to observations than the simplest two models (HadOCC and Diat-HadOCC). As such, we find no robust relationship between model complexity and model skill at capturing global scale distributions of surface $p\mathrm{CO}_2$, DIC and alkalinity. The biologically simpler models are shown to generally best capture the depth profiles of DIC and alkalinity in the oceanographic regions of the North Atlantic and Equatorial Pacific (Figs. 5–6), possibly because their biological export production can more easily be tuned to maintain the observed vertical gradients.

There are however ocean biogeochemical fields where models of greater biological complexity tend to equate to improved model skill. ERSEM, the most complex model assessed, best captures the observed global annual spatial patterns in DIN both in terms of spatial correlation coefficient and standard deviation (Fig. 2). At monthly resolution ERSEM global DIN fields consistently have the highest correlation coefficients however field standard deviations are not always the closest to observations (Fig. S5). It should however be noted that all models have relatively high correlation coefficients for DIN. In addition the annual and monthly global correlation coefficients of the PlankTOM models are shown to be closest to observations for chlorophyll and primary production fields (Fig. 3 and Table 4). These PlankTOM models do not consistently produce the annual chlorophyll and primary production field standard deviations closest to observations (Table 4) however at monthly resolution their field standard deviations are the most consistent across models (Supplement Fig. S5).

The comparison of depth profiles shows that despite all models being initialised from the same observational fields, there is quite a lot of divergence even at depths of 1000 m. In some cases, such as alkalinity in the Southern Ocean (Fig. 6), all models have a similar systematic bias compared to observations. This is suggestive of the influence of discrepancies within the physical ocean model. That is, the ocean biogeochemistry may be influenced to a greater extent by the physical ocean model and hence there is a common response across models. For alternative fields such as DIN in the Southern Ocean and Equatorial Pacific (Supplement Fig. S7), however, models have both positive and negative biases compared to observations suggestive of a greater relative role of the OBGC model than the physical model.

It is clear that more biologically complex models are required to more completely assess the impacts of environmental change on marine ecosystems. By representing processes that are not present in simpler models, the more complex models also tend to represent additional factors such as climatically-active gases (e.g. DMS, N_2O). Assessment of such representations however fell outside the scope of this paper. Models of intermediate complexity (e.g. Diat-HadOCC and MEDUSA-2) are shown in this inter-comparison to reproduce large scale ocean biogeochemistry features relatively well, yet minimise computational cost and have sufficient biological complexity to allow important ESM questions to be explored, including those that require an explicit iron cycle (e.g. ocean iron fertilisation).

It should be noted that models implemented within the NEMO physical ocean framework prior to this inter-comparison project had an advantage over those new to this framework. This is a somewhat unavoidable consequence of what is also one of this inter-comparison study's main strengths, namely that the models were adapted to use the same ocean physics framework. Specifically, the HadOCC and MEDUSA-2 models that were previously implemented within NEMO v3.2 were "familiar" with this ocean model's configuration and flaws. Meanwhile, the ERSEM model, which previously had limited use within the context of the global open ocean, had a distinct disadvantage. Linked to this is the question of how dependent the results found were on parameter settings. Although model developers were afforded a limited opportunity to tune parameters, given further time to tune one would expect improved performance, especially for those models that had not been previously implemented within NEMO v3.2.

The rationale for the chosen fields of intercomparison was, as stated previously, that they are common across all models and are key facets of global marine biogeochemistry. It could however be argued that these bulk fields were insufficient to adequately assess all models and in particular the most complex models. Further analysis, beyond the scope of this paper will undertake as thorough an analysis of the biological components as each model will support. Specifically this will aim to establish if a bottom-up approach to model skill assessment focused on relationships between properties (e.g. Vetter et al., 2008) can identify differences in performance related to the OBGC model complexity.

Finally although computational cost is discussed as a pragmatic driver of OBGC model selection, it should be noted that computer power is continuously increasing and the intercomparison results presented here may differ for an alternative spatial resolution ocean grid requiring greater computational resources. In addition, ongoing efforts to transport passive ocean tracers on degraded spatial scales (e.g. Levy et al., 2012) have the potential to result in computational savings that would realistically permit the implementation of higher complexity OBGC models within ESMs.

5 Conclusions

The 6 ocean biogeochemical models analysed within this inter-comparison cover a large range of ecosystem complexity (from 7 tracers in HadOCC to 57 in ERSEM), and therefore result in a range of approximately 5 in computational costs (from increasing the cost of the physical ocean model by a factor of 2 to a factor of 10). Results suggest little evidence that higher biological complexity implies better model performance in reproducing observed global-scale bulk properties of ocean biogeochemistry.

One priority for the next generation of Earth System Models (CMIP6) is to enhance model resolution in the hope that it will resolve some of the existing biases in climate models. This puts pressure on the computing time available for representing biological complexity. Our results suggest that intermediate complexity models (such as MEDUSA-2 and Diat-HadOCC) offer a good compromise between the representation of biological complexity (through their inclusion of an iron cycle) and computer time, given their relatively good performance in reproducing bulk properties. However, intermediate complexity models are limited in the detail to which they can address climate feedbacks and it may be that more complex models can in future provide additional insight, based on ongoing measurements and data syntheses.

The quest for increasing resolution in ESMs is unlikely to end soon, as the resolution needed to resolve eddies in the ocean ($1/8^{\circ}$ or less) needs to be achieved before important improvements in representing climate dynamics are achieved. Most ESMs being developed for the next CMIP phase will have a grid of $1/2$ to $1/4^{\circ}$. Even with increasing computational power and schemes for accelerating transport of passive tracers (Levy et al., 2012) available, other priorities (e.g. ensemble simulations for risk assessments) may still make it difficult to prioritise the representation of biogeochemical complexity in ESMs. In order to achieve scientific progress on important questions of the interactions between marine biogeochemistry and climate, it is thus important that lower resolution ESMs that prioritise biogeochemical complexity are maintained and used in CMIP exercises in parallel to higher resolution models. Only with a dual low and high resolution strategy can we ensure that the priorities of improving climate dynamics and those of scientific exploration can be achieved. Such a strategy would also help support a closer integration between the assessment of climate change science and that of climate change impacts, and help ensure more integration between IPCC's working groups.

The Supplement related to this article is available online at doi:10.5194/bgd-11-10537-2014-supplement.

Acknowledgements. This work was funded by the UK Natural Environmental Research Council Integrated Marine Biogeochemical Modelling Network to Support UK Earth System Research (i-MarNet) project and the UK Met Office. MFR was partially funded by the EC FP7 GreenSeas project.

References

Barange, M., Merino, G., Blanchard, J. L., Scholtens, J., Harle, J., Allison, E. H., Allen, J. I., Holt, J., and Jennings, S.: Impacts of climate change on marine ecosystem production in societies dependent on fisheries, Nat. Clim. Change, 4, 211–216, doi:10.1038/NCLIMATE2119, 2014.

Baretta, J. W., Ebenhoh, W., and Ruardij, P.: The European Regional Seas Ecosystem Model, a complex marine ecosystem model, Neth. J. Sea Res., 33, 233–246,1995.

Behrenfeld, M. J. and Falkowski, P. G.: Photosynthetic rates derived from satellite-based chlorophyll concentration, Limnol. Oceanogr., 42, 1–20, 1997.

Blackford, J. C.: An analysis of benthic biological dynamics in a North Sea ecosystem model, J. Sea Res., 38, 213–230, 1997.

Blackford, J. C., Allen, J. I., and Gilbert, F. J.: Ecosystem dynamics at six contrasting sites: a generic modelling study, J. Marine Syst., 52, 191–215, 2004.

Bopp, L., Resplandy, L., Orr, J. C., Doney, S. C., Dunne, J. P., Gehlen, M., Halloran, P., Heinze, C., Ilyina, T., Séférian, R., Tjiputra, J., and Vichi, M.: Multiple stressors of ocean ecosystems in the 21st century: projections with CMIP5 models, Biogeosciences, 10, 6225–6245, doi:10.5194/bg-10-6225-2013, 2013.

Braconnot, P., Harrison, S. P., Kageyama, M., Bartlein, P. J., Masson-Delmotte, V., Abe-Ouchi, A., Otto-Bliesner, B., and Zhao, Y.: Evaluation of climate models using palaeoclimatic data, Nat. Clim. Change, 2, 417–424, 2012.

Buesseler, K. O. and Boyd, P. W.: Will ocean fertilisation work?, Science, 300, 67–68, 2003.

Buitenhuis, E., Le Quéré, C., Aumont, O., Beaugrand, G., Bunker, A., Hirst, A., Ikeda, T., O'Brien, T., Piontkovski, S., and Straile, D.: Biogeochemical fluxes through mesozooplankton, Global Biogeochem. Cy., 20, GB2003, doi:10.1029/2005GB002511, 2006.

Buitenhuis, E., Rivkin, R., Sailley, S., and Le Quere, C.: Biogeochemical fluxes through microzooplankton, Global Biogeochem. Cy., 24, GB4015, doi:10.1029/2009GB003601, 2010.

Buitenhuis, E. T., Vogt, M., Moriarty, R., Bednaršek, N., Doney, S. C., Leblanc, K., Le Quéré, C., Luo, Y.-W., O'Brien, C., O'Brien, T., Peloquin, J., Schiebel, R., and Swan, C.: MAREDAT: towards a world atlas of MARine Ecosystem DATa, Earth Syst. Sci. Data, 5, 227–239, doi:10.5194/essd-5-227-2013, 2013.

Carr, M.-E., Friedrichs, M. A. M., Schmeltz, M., Aita, M. N., Antoine, D., Arrigo, K. R., Asanuma, I., Aumont, O., Barber, R., Behrenfeld, M., Bidigare, R., Buitenhuis, E. T., Campbell, J., Ciotti, A., Dierssen, H., Dowell, M., Dunne, J., Esaias, W., Gentili, B., Gregg, W., Groom, S., Hoepffner, N., Ishizaka, J., Kameda, T., Le Quéré, C., Lohrenz, S., Marra, J., Mélin, F., Moore, K., Morel, A., Reddy, T. E., Ryan, J., Scardi, M., Smyth, T., Turpie, K., Tilstone, G., Waters, K., and Yamanaka, Y.: A comparison of global estimates of marine primary production from ocean color, Deep-Sea Res. Pt. II, 53, 741–770, 2006.

Cheung, W. W. L., Sarmiento, J. L., Dunne, J. P., Frölicher, T. L., Lam, V. W. Y., Palomares, M. L. D., Watson, R. and Pauly, D.: Shrinking of fishes exacerbates impacts of global ocean changes on marine ecosystems, Nat. Clim. Change, 3, 254–258, 2012.

Collins, W. J., Bellouin, N., Doutriaux-Boucher, M., Gedney, N., Halloran, P., Hinton, T., Hughes, J., Jones, C. D., Joshi, M., Liddicoat, S., Martin, G., O'Connor, F., Rae, J., Senior, C., Sitch, S., Totterdell, I., Wiltshire, A., and Woodward, S.: Development and evaluation of an Earth-System model – HadGEM2, Geosci. Model Dev., 4, 1051–1075, doi:10.5194/gmd-4-1051-2011, 2011.

Condon, R., Duarte, C. M., Pitt, K. A., Robinson, K., Lucas, C. H., Sutherland, K. R., Mianzan, H. W., Bogeberg, M., Purcell, J. E., Decker, M. B., Uye, S., Madin, L. P., Brodeur, R. D., Haddock, S. H. D., Malej, A., Parry, G. D., Eriksen, E., Quiñones, J. Acha, M., Harvey, M., Arthur, J. M., and Graham, W. M.: Recurrent jellyfish blooms are a consequence of global oscillations, P. Natl. Acad. Sci. USA, 110, 1000–1005, 2013.

Cox, P. M., Betts, R. A., Jones, C. D., Spall, S. A., and Totterdell, I. J.: Acceleration of global warming due to carbon-cycle feedbacks in a coupled climate model, Nature, 408, 184–187, 2000.

Friedlingstein, P., Cox, P., Betts, R., Bopp, L., Von Bloh, W., Brovkin, V., Cadule, P., Doney, S., Eby, M., Fung, I., Bala, G., John, J., Jones, C., Joos, F., Kato, T., Kawamiya, M., Knorr, W., Lindsay, K., Matthews, H. D., and Raddatz, T.: Climate–carbon cycle feedback analysis: results from the C4MIP model intercomparison, J. Climate, 19, 3337–3353, 2006.

Garcia, H. E., Locarnini, R. A., Boyer, T. P., Antonov, J. I., Baranova, O. K., Zweng, M. M., and Johnson, D. R.: World Ocean Atlas 2009, Volume 3: Dissolved Oxygen, Apparent Oxygen Utilization, and Oxygen Saturation, edited by: Levitus, S., NOAA Atlas NESDIS 70, US Government Printing Office, Washington DC, 344 pp., 2010a.

Garcia, H. E., Locarnini, R. A., Boyer, T. P., Antonov, J. I., Zweng, M. M., Baranova, O. K., and Johnson, D. R.: World Ocean Atlas 2009, Volume 4: Nutrients (Phosphate, Nitrate, Silicate), edited by: Levitus, S., NOAA Atlas NESDIS 71, US Government Printing Office, Washington DC, 398 pp., 2010b.

Gruber, N.: Warming up, turning sour, losing breath: ocean biogeochemistry under global change, Philos. T. R. Soc. A, 369, 1980–1996, 2011.

Halloran, P. R., Bell, T. G., and Totterdell, I. J.: Can we trust empirical marine DMS parameterisations within projections of future climate?, Biogeosciences, 7, 1645–1656, doi:10.5194/bg-7-1645-2010, 2010.

Hewitt, H. T., Copsey, D., Culverwell, I. D., Harris, C. M., Hill, R. S. R., Keen, A. B., McLaren, A. J., and Hunke, E. C.: Design and implementation of the infrastructure of HadGEM3: the next-generation Met Office climate modelling system, Geosci. Model Dev., 4, 223–253, doi:10.5194/gmd-4-223-2011, 2011.

Hunke, E. C. and Lipscomb, W. H.: CICE: The Los Alamos Sea Ice Model, Documentation and Software User's Manual, Version 4.0, Los Alamos National Laboratory Tech. Rep. LA-CC-06, 2008.

Jackson, D. A., Peres-Neto, P. R., and Olden, J. D.: What controls who is where in freshwater fish communities – the roles of biotic, abiotic, and spatial factors, Can. J. Fish. Aquat. Sci., 58, 157–170, 2001.

Jolliff, J. K., Kindle, J. C., Shulman, I., Penta, B., Friedrichs, M. A. M., Helber, R., and Arnone, R. A.: Summary diagrams for coupled hydrodynamic-ecosystem model skill assessment, J. Marine Syst., 76, 64–82, 2009.

Key, R. M., Kozyr, A., Sabine, C. L., Lee, K., Wanninkhof, R., Bullister, J. L., Feely, R. A., Millero, F. J., Mordy, C., and Peng, T.-H.: A global ocean carbon climatology: results from Global Data Analysis Project (GLODAP), Global Biogeochem. Cy., 18, GB4031, doi:10.1029/2004GB002247, 2004.

Kheshgi, H. S.: Sequestering atmospheric carbon dioxide by increasing ocean alkalinity, Energy, 20, 915–922, 1995.

Large, W. and Yeager, S.: The global climatology of an interannually varying air–sea flux data set, Clim. Dynam., 33, 341–364, 2009.

Le Quéré, C., Harrison, S. P., Prentice, I. C., Buitenhuis, E. T., Aumont, O., Bopp, L., Claustre, H., Da Cunha, L. C., Geider, R., Giraud, X., Klaas, C., Kohfeld, K. E., Legendre, L., Manizza, M., Platt, T., Rivkin, R. B., Sathyendranath, S., Uitz, J., Watson, A. J., and Wolf-Gladrow, D.: Ecosystem dynamics based on plankton functional types for global ocean biogeochemistry models, Glob. Change Biol., 11, 2016–2040, doi:10.1111/j.1365-2486.2005.1004.x, 2005.

Lévy, M., Resplandy, L., Klein, P., Capet, X., and Ethé, C.: Grid degradation of submesoscale resolving ocean models: benefits for offline passive tracer transport, Ocean Model., 48, 1–9, 2012.

Madec, G.: NEMO Reference Manual, Ocean Dynamic Component: NEMO–OPA, Note du Pôle de modélisation, Technical Report 27, Institut Pierre Simon Laplace, France, ISSN No. 1288–1619, 2008.

O'Reilly, J. E., Maritorena, S., Mitchell, B. G., Siegal, D. A., Carder, K. L., Garver, S. A., Kahru, M., and McClain, C.: Ocean color chlorophyll algorithms for SeaWiFS, J. Geophys. Res., 103, 24937–24953, 1998.

Palmer, J. R. and Totterdell, I. J.: Production and export in a global ocean ecosystem model, Deep-Sea Res. Pt. I, 48, 1169–1198, 2001.

Reid, P. C., Fischer, A. C., Lewis-Brown, E., Meredith, M. P., Sparrow, M., Andersson, A. J., Antia, A., Bates, N. R., Bathmann, U., Beaugrand, G., Brix, H., Dye, S., Edwards, M., Furevik, T., Gangstø, R., Hátún, H., Hopcroft, R. R., Kendall, M., Kasten, S., Keeling, R., Le Quéré, C., Mackenzie, F. T., Malin, G., Mauritzen, C., Ólafsson, J., Paull, C., Rignot, E., Shimada, K., Vogt, M., Wallace, C., Wang, Z., and Washington, R.: Chapter 1. Impacts of the oceans on climate change, Adv. Mar. Biol., 56, 1–150, 2009.

Siddorn, J. R., Allen, J. I.,Blackford, J. C., Gilbert, F. J., Holt, J. T., Holt, M. W., Osborne, J. P., Proctor, R., and Mills, D. K.: Modelling the hydrodynamics and ecosystem of the north-west European continental shelf for operational oceanography, J. Marine Syst., 65, 417–429, doi:10.1016/j.jmarsys.2006.01.018, 2007.

Takahashi, T., Sutherland, S. C., Wanninkhof, R. Sweeney, C., Feely, R. A., Chipman, D. W., Hales, B., Friederich, G., Chavez, F., Sabine, C., Watson, A., Bakker, D. C. E., Schuster, U., Metzl, N., Yoshikawa-Inoue, H., Ishii, M. Midorikawa, T., Nojiri, Y., Kortzinger, A., Steinhoff, T., Hoppema, M., Olafsson, J., Arnarson, T. S., Tillbrook, B., Johannessen, T., Olsen, A., Bellerby, R., Wong, C. S., Delille, B., Bates, N. R., and de Baar, H. J. W.: Climatological mean and decade change in surface ocean $p\mathrm{CO}_2$, and net sea–air CO_2 flux over the global oceans, Deep-Sea Res. Pt. II, 56, 554–577, doi:10.1016/j.dsr2.2008.12.009, 2009.

Taylor, K. E.: Summarizing multiple aspects of model performance in a single diagram, J. Geophys. Res., 106, 7183–7192, 2001.

Vetter, M., Churkina, G., Jung, M., Reichstein, M., Zaehle, S., Bondeau, A., Chen, Y., Ciais, P., Feser, F., Freibauer, A., Geyer, R., Jones, C., Papale, D., Tenhunen, J., Tomelleri, E., Trusilova, K., Viovy, N., and Heimann, M.: Analyzing the causes and spatial pattern of the European 2003 carbon flux anomaly using seven models, Biogeosciences, 5, 561–583, doi:10.5194/bg-5-561-2008, 2008.

Westberry, T., Behrenfeld, M. J., Siegel, D. A., and Boss, E.: Carbon-based primary productivity modeling with vertically resolved photoacclimation, Global Biogeochem. Cy., 22, GB2024, doi:10.1029/2007GB003078, 2008.

Yool, A., Popova, E. E., and Anderson, T. R.: Medusa-1.0: a new intermediate complexity plankton ecosystem model for the global domain, Geosci. Model Dev., 4, 381–417, doi:10.5194/gmd-4-381-2011, 2011.

Yool, A., Popova, E. E., and Anderson, T. R.: MEDUSA-2.0: an intermediate complexity biogeochemical model of the marine carbon cycle for climate change and ocean acidification studies, Geosci. Model Dev., 6, 1767–1811, doi:10.5194/gmd-6-1767-2013, 2013.

Table 1. Biogeochemical cycles represented in each candidate model.

	HadOCC	Diat-HadOCC	MEDUSA-2	PlankTOM6	PlankTOM10	ERSEM
N	√	√	√	√	√	√
P					√	√
Si		√	√	√	√	√
Fe		√	√	√	√	√
C	√	√	√	√	√	√
Alkalinity	√	√	√	√	√	√
O_2	√	√	√	√	√	√

Table 2. Composition of the marine ecosystems represented in each candidate model, along with the total number of biogeochemical tracers (including those detailed in Table 1).

	HadOCC	Diat-HadOCC	MEDUSA-2	PlankTOM6	PlankTOM10	ERSEM
Generic Phytoplankton	√	√		√	√	
Diatoms		√	√	√	√	√
Large Phytoplankton						√
Picophytoplankton			√		√	√
Coccolithophores				√	√	√
N_2 fixers					√	
Flagellates						√
Phaeocystis					√	
Generic Zooplankton	√	√				
Microzooplankton			√	√	√	√
Mesozooplankton			√	√	√	√
Macrozooplankton					√	
Heterotrophic Nanoflagellates						√
Prokaryotes				√	√	√
Tracers	7	13	15	25	39	57

Table 3. Model-observation correlation coefficients (*R*) and standard deviations normalised by the standard deviation of observations (σ) for all examined annual surface fields and depth integrated primary productivity. Colours indicate model ranking and are organised through the worst performing model in red to the best performing model in dark blue (through orange, yellow, green and light and dark blue).

Model	**pCO_2**		**DIN**		**Chl.**		**Oxygen**		**Alkalinity**		**DIC**		**Primary Production**	
	R	**σ**	***R***	**σ**	***R***	**σ**	***R***	**σ**	***R***	**σ**	***R***	**σ**	***R***	**σ**
HadOCC	0.68	1.92	0.88	1.20	0.30	0.68	0.99	1.07	0.91	1.19	0.93	1.18	0.19	0.92
Diat-HadOCC	0.54	1.77	0.90	1.20	0.15	2.65	0.99	1.08	0.91	1.19	0.93	1.13	0.13	1.51
MEDUSA-2	0.64	1.56	0.85	1.21	0.36	0.40	0.99	1.02	0.88	1.14	0.92	1.17	0.64	1.10
PlankTOM6	0.34	1.03	0.79	1.20	0.32	1.08	0.99	1.05	0.70	0.88	0.75	0.96	0.47	0.61
PlankTOM10	0.29	0.94	0.88	1.19	0.50	0.43	0.99	1.04	0.58	1.16	0.65	1.08	0.53	0.74
ERSEM	0.01	2.04	0.94	0.95	0.04	0.91	0.98	0.97	0.84	1.18	0.86	1.07	-0.08	1.12
Range	0.67	1.09	0.15	0.26	0.46	2.25	0.01	0.11	0.33	0.31	0.28	0.23	0.72	0.90

Title Page
Abstract Introduction
Conclusions References
Tables Figures
◀| |▶
◀ ▶
Back Close
Full Screen / Esc

Printer-friendly Version
Interactive Discussion

Table 4. Computational cost of each candidate model when coupled to the ocean component of HadGEM3, relative to a physics-only simulation with the same ocean model (ORCA1.0L75). A cost of 2.0 indicates that adding the biogeochemistry model doubles total simulation cost. Timings are shown for simulations carried-out on 128 and 256 processors of an IBM Power7 machine.

Model	Cost (128 processors)	Cost (256 processors)
HadOCC	1.75	1.48
Diat-HadOCC	2.36	1.88
MEDUSA-2	2.73	2.10
PlankTOM6	5.11	3.52
PlankTOM10	7.74	4.90
ERSEM	10.36	6.87

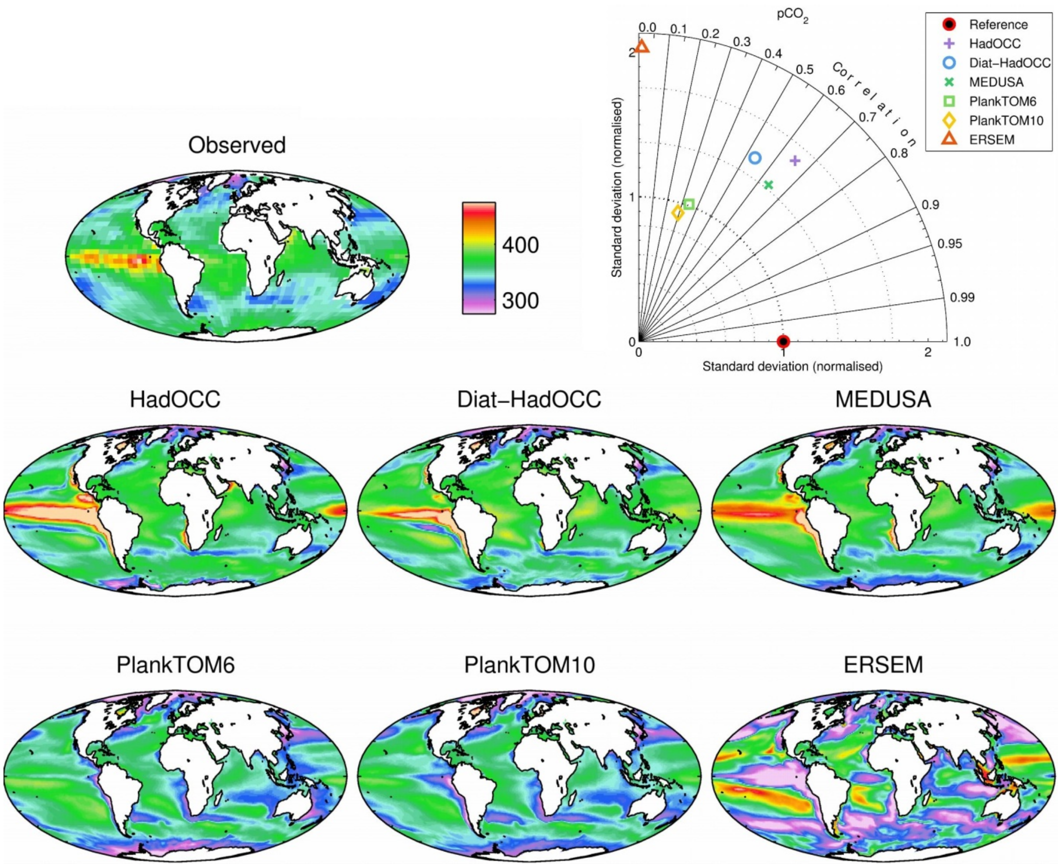

Figure 1. Observational (Takahashi et al., 2009; top left) and modelled annual average surface ocean $p\mathrm{CO}_2$ (μatm) for year 2000.

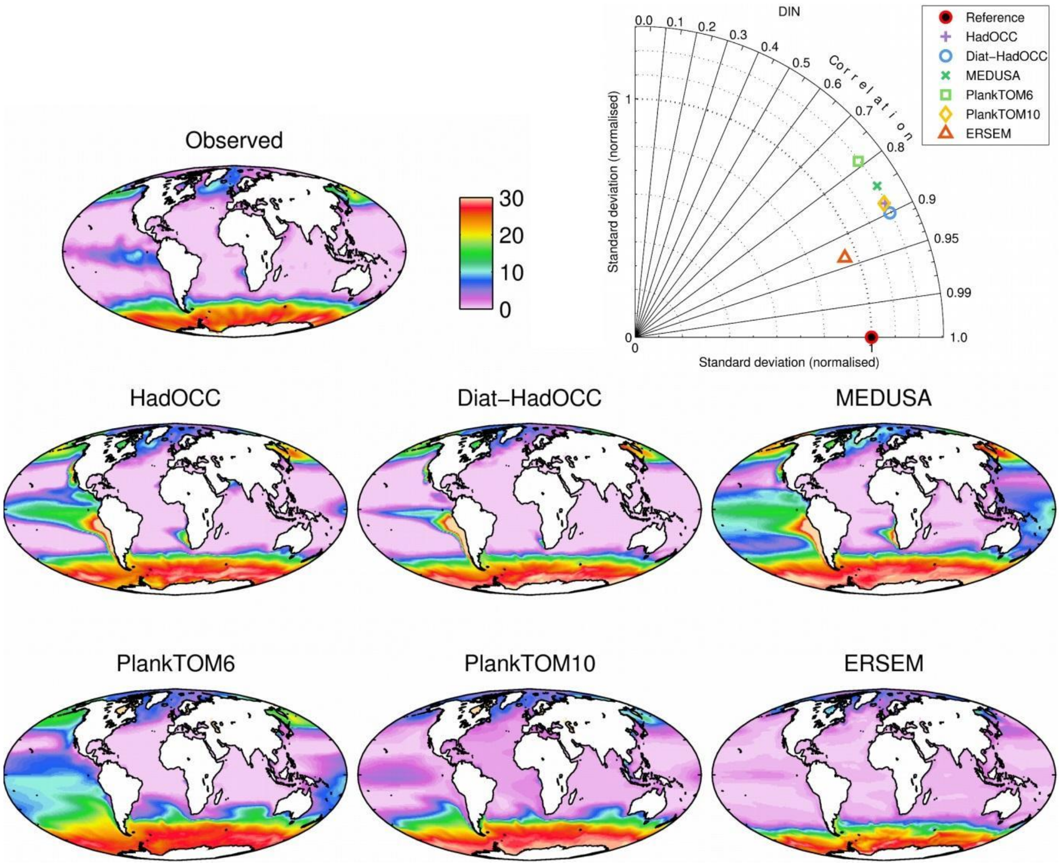

Figure 2. Observational (World Ocean Atlas, 2009; top left) and modelled annual average surface ocean Dissolved Inorganic Nitrogen (mmol $\mathrm{m^{-3}}$) for the period 2000–2004.

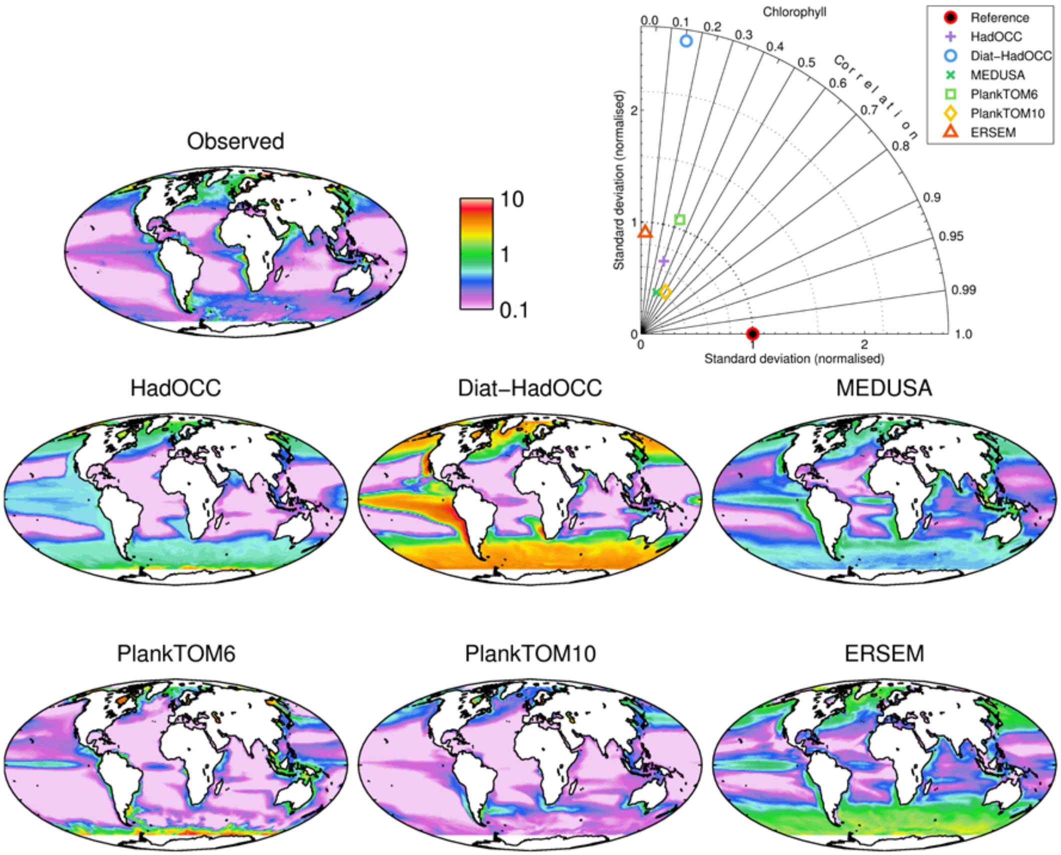

Figure 3. Observational (SeaWiFS; top left) and modelled annual average surface ocean chlorophyll ($\text{mg}\,\text{m}^{-3}$) for the period 2000–2004. To avoid biasing the plots, observational data and model output are only shown for regions in which all months were represented at least once across all of the sampled years.

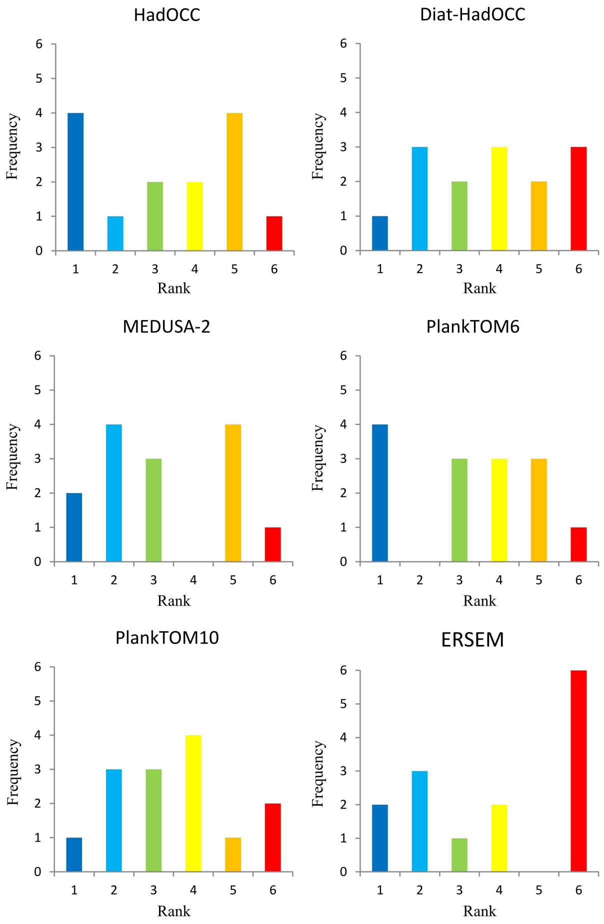

Figure 4. Frequency distributions of best- to worst-performances for each model, in terms of correlation coefficients and normalised standard deviations or annual surface fields and depth integrated primary productivity. Colours follow those of Table 3.

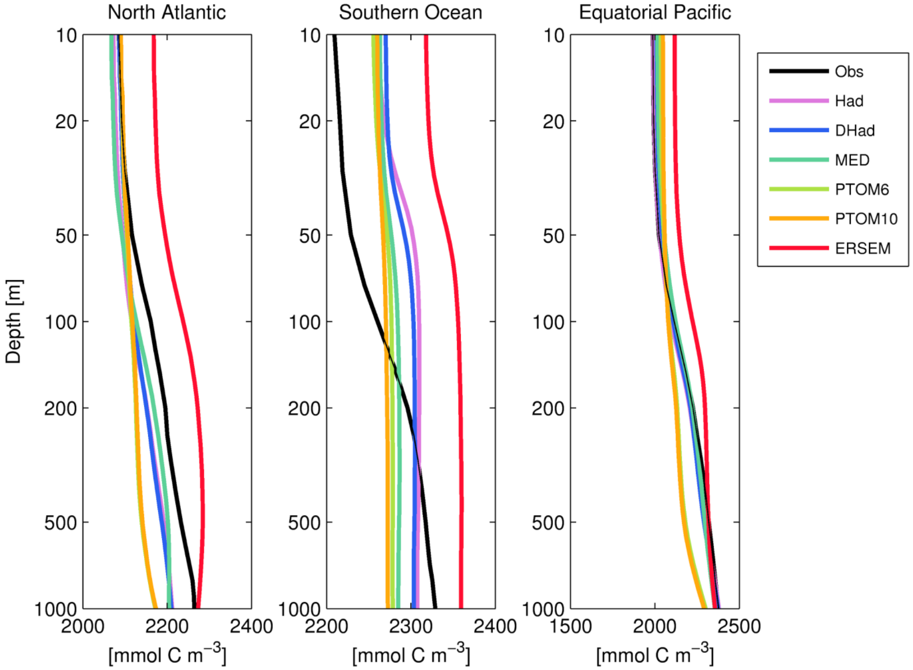

Figure 5. Observed (black; GLODAP) and modelled profiles of Dissolved Inorganic Carbon (mmol C m^{-3}) in the North Atlantic (0 to 60° N), Southern Ocean (90 to 60° S) and Equatorial Pacific (15° S to 15° N).

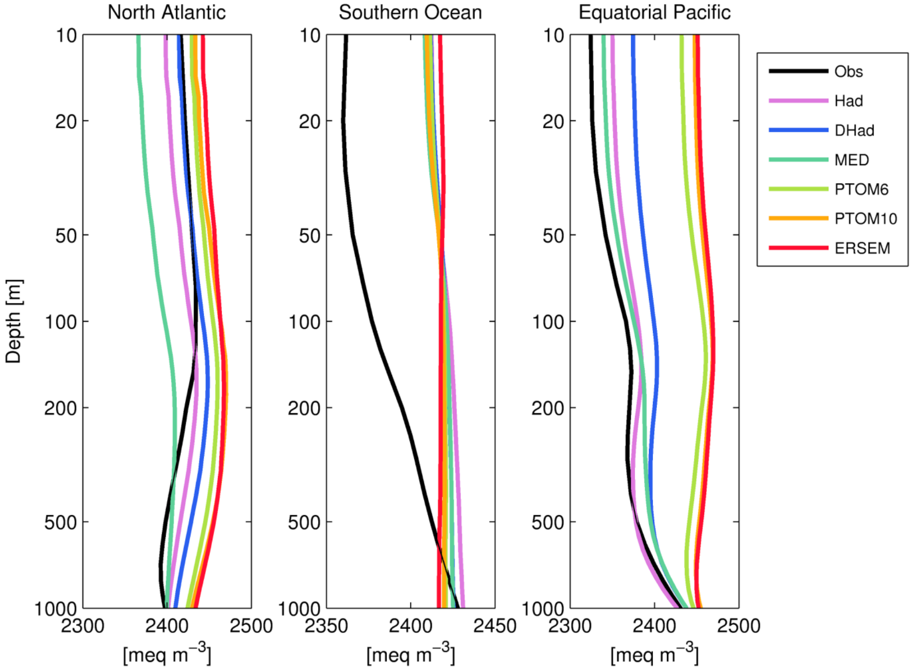

Figure 6. Observed (black; GLODAP) and modelled profiles of alkalinity (meq m^{-3}) in the North Atlantic (0 to 60° N), Southern Ocean (90 to 60° S) and Equatorial Pacific (15° S to 15° N).